Journal of Integrative Agriculture 2026, 25(7): 2936–2949

Available online at ScienceDirect

Journal of Integrative Agriculture



RESEARCH ARTICLE

Multiomics integration identifies regulatory factors underlying reproductive disorders in geese

Qingyuan Ouyang[1, 2*], Cong Lan[3*], Shenqiang Hu[1, 2*], Haizhou Gong[4], Bincheng Tang[1, 2], Qingliang Chen[1, 2], Zhiyu He[1, 2], Junqi Wang[1, 2], Tanze Liu[1, 2], Shangmin Wang[1, 2], Xi Zhang[1, 2], Jiwei Hu[1, 2], Hua He[1, 2], Liang Li[1, 2], Hehe Liu[1, 2], Jiwen Wang[1, 2#]

[1] *State Key Laboratory of Swine and Poultry Breeding Industry, College of Animal Science and Technology, Sichuan Agricultural University, Chengdu 611130, China*

[2] *Farm Animal Genetic Resources Exploration and Innovation Key Laboratory of Sichuan Province, Sichuan Agricultural University, Chengdu 611130, China*

[3] *Engineering Research Center of Animal Disease-Resistance Nutrition Biotechnology of Ministry of Education of China, Animal Nutrtition Institute, Sichuan Agricultural University, Chengdu 611130, China*

[4] *College of Animal Science and Technology, Yangzhou University, Yangzhou 225009, China*

Highlights

- Multi-omic characterization of reproductive disorders (RD): Integrative ovarian anatomical, histological, and transcriptomic profiling reveals the underlying pathogenic mechanisms of RD in geese, establishing a foundational model for studying avian reproductive health.
- Bile acid metabolism as a core driver: Genetic mutations in bile acid metabolism genes disrupt circulating chenodeoxycholic acid (CDCA) levels, directly linking bile acid dysregulation to the pathogenesis of RD.
- CDCA-microbiota axis in RD progression: Elevated CDCA selectively promotes the proliferation of *Romboutsia lituseburensis* in the ileum, demonstrating a causal pathway from host metabolic alteration to gut microbiota dysbiosis and subsequent reproductive impairment.

Abstract

Geese, descendants of migratory birds, have preserved the distinct reproductive and lipid metabolism traits of their wild ancestors. Therefore, compared to other poultry, geese have lower egg production ability and greater susceptibility to fatty liver. Recent research underscores the impact of lipid metabolism disorders on female reproductive health. In this context, we observed reproductive disorders (RD) and lipid metabolism anomalies in certain geese populations. This study systematically elucidated the differences between RD and normal geese at various levels, including genomics, transcriptomics, bile acid metabolomics, and microbiomics, revealing the crucial role of microorganisms. Our study provides a thorough examination of the ovarian anatomical, histological, and transcriptomic profiles between normal and RD geese. Genomic analyses pinpoint mutations in genes associated with bile acid metabolism, highlighting their potential role in RD pathogenesis. The genomic discoveries are substantiated by precise bile acid assays and ileum transcriptome analyses, which expose a significant disruption in bile acid absorption, activation of *FXR*, and an increase in serum chenodeoxycholic acid (CDCA) concentrations within RD geese. Notably, 16S rRNA sequencing uncovers significantly greater beta diversity in the ileum microbiota of RD geese than in the normal group. Both Wilcoxon rank sum test and LEfSe analyses highlighted a marked increase in *Romboutsia* abundance in RD geese. Experimental cultivation of microbiota with CDCA supplementation confirms the impact of CDCA on *Romboutsia lituseburensis* proliferation. Gavage experiments with *R. lituseburensis* elucidate its involvement in primary follicle reduction *via* immune-mediated pathways. Collectively, our multifaceted analysis unravels the intricate involvement of *Romboutsia* in goose RD, offering insights from genetic, physiological, and microbial dimensions. Our findings not only deepen understanding of the etiology of RD in geese but also

Received 10 April 2024; Received in revised form 29 April 2024; Accepted 15 May 2024; Available online 24 May 2024
Qingyuan Ouyang, E-mail: oyqy222@163.com; Cong Lan, E-mail: clarencelan7777@163.com; Shenqiang Hu, E-mail: sqhu2011@163.com; #Correspondence Jiwen Wang, Tel: +86-28-86293073, E-mail: wjw2886166@163.com
* These authors contributed equally to this study.

© 2026 CAAS. Publishing services by Elsevier B.V. on behalf of KeAi Communications Co. Ltd. This is an open access article under the CC BY-NC-ND license (http://creativecommons.org/licenses/by-nc-nd/4.0/). Peer review under responsibility of Editorial Board of *Journal of Integrative Agriculture*.
doi: 10.1016/j.jia.2024.05.030

suggest potential avenues for therapeutic interventions targeting bile acid metabolism and modulation of specific microbiota components.

Keywords: goose, bile acid, gut microbiota, reproduction dysfunction

1. Introduction

The domestication of geese into economically valuable poultry by humans has a rich history, originating from wild species *Anser cygnoides* or *Anser anser*. These domesticated birds have retained several ancestral physiological traits linked to migration, for instance, in reproduction and lipid metabolism. *A. cygnoides* and *A. anser* are particularly noted for their pre-migratory habit of ingesting copious amounts of food, a practice that results in physiological hepatic lipid deposition (Hermier *et al.* 1991) and exhibits an enhanced natural predisposition towards fat accumulation. This trait is now harnessed for the production of fatty liver (Wei *et al.* 2021). Although geese have lost the ability to migrate, their practice of seasonal reproduction is still preserved, which may be linked to their lipid distribution mechanism. The liver and adipose tissue are the primary organs for lipid regulation, synthesis, and homeostasis (Zaefarian *et al.* 2019). Laying performance in poultry largely depends on the transport of liver lipids, and the lower laying frequency in geese is connected to their unique lipid metabolism mechanism. Notably, during domestication and selective breeding, some geese developed reproductive disorders (RD) associated with abnormal lipid metabolism (Ouyang *et al.* 2022).

Lipids participate in oogenesis and oocyte development and serve as a source of energy and substrate for several intracellular processes, playing a role in the establishment of pregnancy, regulation of the maternal-fetal interface, and fetal development (Herrera and Ortega-Senovilla 2010). Hence, lipid metabolism disorders are commonly observed in RD (Dunaif 1997; Broughton and Moley 2017). Polycystic ovary syndrome (PCOS), a pathology that associates anovulation and infertility with various metabolic abnormalities, is one example (Barber *et al.* 2006; Diamanti-Kandarakis and Dunaif 2012; Salva-Pastor 2019). Fatty liver hemorrhagic syndrome in laying hens has been shown to significantly reduce their laying performance. Overfeeding can reduce the laying performance of broiler breeders, which is associated with obesity, liver degeneration, and systemic inflammation (Wei *et al.* 2019; Chen *et al.* 2023). Additionally, the level of laying performance in geese is closely related to the lipid content in the liver and the expression of related genes (Ouyang *et al.* 2022).

Microorganisms have been widely reported to participate in the regulation of female poultry reproductive functions (Han *et al.* 2022), with certain microbes demonstrated to enhance reproductive ability (Wang *et al.* 2020), while others have been identified as detrimental to these characteristics (Yuan *et al.* 2022). Recently, the involvement of microorganisms in the regulation of host metabolism and female reproductive disorders has been associated with bile acid metabolism (Qi *et al.* 2019; Li *et al.* 2023; Tang *et al.* 2023). Bile acids, substances related to fat digestion, are intimately linked with the development of RD (Yang *et al.* 2021; Yu *et al.* 2023). Synthesized in the liver *via* classical or alternative pathways, 95% of bile acids are absorbed at the terminal ileum, profoundly influencing the foregut microbial community (Wahlstrom *et al.* 2016; Collins *et al.* 2023). This study aims to elucidate the patterns of change in RD in geese across genetic, metabolic (including bile acids), and gut microbiota axes. By revealing the complex interplay between host metabolism, gut microbial composition, and reproductive processes, we seek to clarify the underlying mechanisms driving RD (Fig. 1) and to decode the interaction between host phenotype and gut microbiota.

2. Materials and methods

2.1. Animals

First, a total of 236 female geese (Sichuan white goose×Landes goose F_2 resource population) were raised at the Waterfowl Breeding Experimental Site of Sichuan Agricultural University (Ya'an, Sichuan, China). Detailed individual egg-laying records were meticulously maintained. The body weight of all individuals was recorded at 0, 2, 4, 6, 8, 10, 14, 18, 22, 26, 30, and 43 wk of age. Blood samples from 236 female geese at 10 wk were obtained by venipuncture from the vein under the wing. The collected blood was divided into two aliquots: one for serum separation and the other for DNA extraction. Geese that had not initiated egg laying by the age of 365 d were categorized as experiencing RD. Simultaneously, a subset of 5 geese from the RD and normal groups were humanely euthanized to obtain ovarian stroma, liver, and ileum for transcriptome sequencing. Additionally, 3 female geese in the normal group at the peak laying stage were euthanized to collect ileum contents for *in vitro* cultivation of ileum chyme microbiota. A total of 60 geese with similar weight at the age of 70 d were used for inoculation with *Romboutsia lituseburensis*, with each group consisting of 30 geese.

2.2. Analysis of serum index

The assessment of serum glucose (GLU) concentration involved the utilization of the Glucose Assay Kit (Solarbio, Beijing, China), executed according to established protocols. Insulin, cholesterol (CH), triglycerides (TG), very low-density lipoprotein cholesterol (VLDL-C), high-density lipoprotein cholesterol (HDL-C), IgA, IgG, IgM, and LPS were quantified using specialized ELISA assay kits specifically designed for geese (Huding, Shanghai, China). The procedures were meticulously carried out in strict accordance with the manufacturer's instructions. Student's *t*-test was used for group comparisons, and Prism 10 software was used for visualizing results.

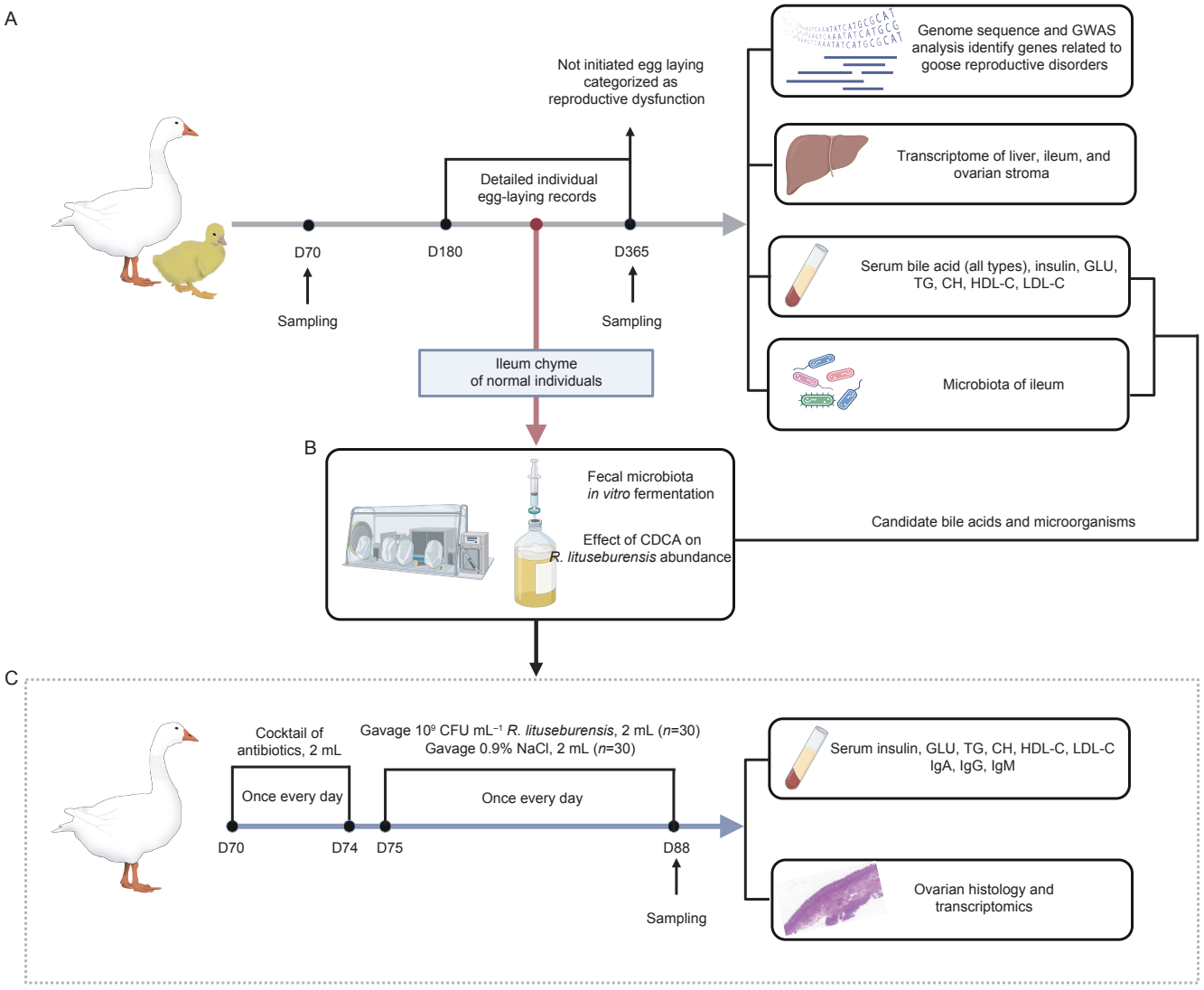


Fig. 1 Overview of experiment design. A, initially, we pinpoint genes linked to reproductive disorders (RDs) within the population by analyzing genomic and transcriptomic sequencing data. Meanwhile, we conduct untargeted metabolomic profiling to examine serum bile acids and identify ileal differentially abundant microbiota through 16S rRNA sequencing. B, we conduct *in vitro* experiments to validate the impact of candidate bile acids on the abundance of signature ileal microbiota, providing evidence to establish the relationship between bile acids and microbiota. C, moreover, we undertake additional gavage experiments with candidate strains in a separate population to substantiate their effects on serum metabolic indicators and ovarian development. GWAS, genome-wide association study; GLU, serum glucose; TG, triglycerides; CH, cholesterol; HDL-C, high-density lipoprotein cholesterol; LDC-C, low-density lipoprotein cholesterol; CDCA, chenodeoxycholic acid.

2.3. Quantitative analysis of serum bile acid

The assessment of serum bile acids involved the analysis of 10 samples from the normal group and 10 samples from the RD group. Sikaiao Biomedical Technology Co., Ltd. (Beijing, China) meticulously conducted the entire process, encompassing sample preparation, calibration standard curve construction, and UHPLC-MS/MS analysis. Raw data were rigorously processed using MassHunter Workstation software (vB.08.00, Agilent), adhering to default parameters and manual inspection for both qualitative and quantitative accuracy of individual compounds. The integration of peak areas for each compound across all samples was carried out with utmost precision. Ten-point calibration curves were meticulously generated by correlating the peak area ratio of each compound to the internal standard against the concentration of each compound. Subsequently, the concentrations (C, μg mL^{-1}) of bile acids within the prepared samples were automatically quantified. These quantified values underwent further quantitative calculation for serum samples using an Excel-based approach, according to the formula: Content (serum, ng mL^{-1})=C×1,000/2, where C represents the concentration quantified within the prepared sample (μg mL^{-1}). This rigorous analytical methodology, guided by both technological precision and established formulas, ensured the accurate quantification of serum bile acid levels. Student's-test was used for group comparisons, and Prism 10 software was used for visualizing results.

2.4. Transcriptome analysis

The Trizol Kit (Invitrogen, Santa Clara, CA, USA) was used to extract the total RNA of tissue according to the manufacturer's instructions. The qualified RNA samples were used for library construction. The mRNA libraries were sequenced by Novogene Co., Ltd. (Beijing, China) using Nova-PE150 (Illumina, San Diego, CA, USA). The clean reads were obtained after filtration of low-quality reads using standard quality control by FastQC software. Clean reads were mapped to the Sichuan white goose reference genome (PRJNA801885) using HISAT2 (v2.2.1) software (Kim *et al.* 2015). The output sequence alignment/map (SAM) file was converted to a binary alignment/map (BAM) file and sorted using SAMtools (v1.10) (Li *et al.* 2009). Subsequently, the expression of each transcript was calculated by featureCounts (v1.6.0) (Liao *et al.* 2014). DESeq2 was used to identify the differentially expressed genes (DEGs) among different groups; the screening criteria were $|\log_2$ FoldChange$|>1$ and P-value<0.05. Functional analysis used KOBAS 3.0 online (http://kobas.cbi.pku.edu.cn/kobas3/?t=1, accessed on 2 February 2023) (Bu *et al.* 2021). The STRING 11.5 database (http://string-db.org/) was used to identify the relationships among DEGs, and Cytoscape software (v3.7.1) was used for network visualization.

2.5. Genome-wide association study analysis (GWAS)

The DNeasy Blood and Tissue Kit (Qiagen, Valencia, CA, USA) was used to extract genomic DNA from blood. In total, 236 female geese were resequenced on the Illumina NovaSeq 6000 platform by Novogene Co., Ltd. (Tianjin, China). We set the sequencing depth of each sample at more than 20×. The FastQC software was used to assess the raw data. Based on the quality of the raw data, the NGS QC Toolkit (Patel and Jain 2012) was used to conduct quality control on the original sequencing data, and residual primers and adapter sequences were removed. Meanwhile, sequencing bases with less than 70% read length and quality scores greater than 20 were retained; bases failing these criteria were removed. Subsequently, the quality-controlled data were aligned to the chromosomes of the Sichuan white goose genome we assembled (PRJNA801885) using the BWA-MEM software (Li 2013) with the parameter 'bwa mem -k 40 -M -R'. The resulting SAM file was converted to BAM format using SAMtools (Li *et al.* 2009), and unmapped and non-uniquely mapped reads were filtered. Variant calling was performed following the best practice workflow recommended by GATK (v4.1.7.0). Briefly, GATK HaplotypeCaller with the GVCF model was used to call SNPs for each sample. Joint genotyping was performed using the combined GVCF file to obtain comprehensive variants across all samples. Filtering parameters were as follows: QD<2.0 | | MQ<40.0 | | FS>60.0 | | SOR>3.0 | | MQRankSum<–12.5 | | ReadPosRankSum<–8.0. SNPs with missingness>0.1, sequencing depth<4, minor allele frequency (MAF)<0.05, or genotype quality (GQ)<5 were excluded, and the remaining SNPs were used for subsequent analysis. We used the identified SNPs from all geese for GWAS analysis. GWAS was performed using the univariate linear mixed model (LMM) in the Genome-wide Efficient Mixed-model Association (GEMMA) software (Zhou and Stephens 2012). The CMplot R package was used to visualize the Manhattan plot of GWAS results. A significance threshold of $1e^{-6}$ was set for trait-associated variants, and the variant information was annotated with gene names.

2.6. 16S rRNA amplicons sequencing and analysis

For microbial diversity analysis, the ileum chyme underwent 16S rRNA sequencing. Microbial DNA was meticulously extracted using the E.Z.N.A. Stool DNA Kit (Omega Bio-Tek, Norcross, GA), following the manufacturer's instructions. The V3–V4 hypervariable regions of bacterial 16S rRNA genes were amplified using the thermocycler PCR system with primers 338-F (5′-ACTCCTACGGGAGGCAGCAG-3′) and 806-R (5′-GGACTACNNGGGTATCTAAT-3′). PCR products exhibiting the correct size and appropriate concentration were used for subsequent experiments. Ultimately, 11 samples were designated for sequencing. The obtained products underwent purification, pooling, and DNA library construction, culminating in sequencing *via* the Illumina MiSeq platform. To ensure quality, the sequencing data underwent meticulous quality control. QIIME2 software (v2023.5) (Bolyen *et al.* 2019) was employed for processing and assignment of these assembled reads. The denoise-paired method in DADA2 was applied to identify amplicon sequence variants (ASVs). Annotation of results utilized the SILVA 138 database (Quast *et al.* 2013). The boot and stats packages in R (v3.3.1) were used to identify differences in alpha diversity, beta diversity, and microbial diversity between the two groups by Wilcoxon rank-sum test. Meanwhile, differences in microbial composition between the groups were assessed using LEfSe (Segata *et al.* 2011), employing screening criteria of LDA score>3 and P<0.05. The Linear Discriminant Analysis Effect Size (LEfSe) software was employed for linear discriminant analysis (LDA) based on taxonomic composition (from phylum to genus) to analyze samples under different grouping conditions. Microorganisms with LDA>3 and a P-value<0.05 were considered key differential microbes.

2.7. *In vitro* cultivation of ileum chyme microbiota

To investigate microbial responses and metabolic dynamics to varying CDCA concentrations, ileum chyme microbiota was cultured *in vitro*. The detailed experimental procedures have been described previously (Martin *et al.* 2018). Fresh ileum chyme (10%, w/v) was homogenized in anaerobic phosphate-buffered saline (PBS; 0.1 mol L^{-1}, pH 7.4) at 460 beats min^{-1} for 120 s, thus generating ileum slurries. Each fermentation vessel was inoculated with 6 mL of fecal slurry into 53 mL of basal medium to a final concentration of 10% (v/v). The composition of the basal medium per liter included: 2 g peptone (BBI LIFE SCIENCES, Shanghai, China), 2 g yeast extract (BBI LIFE SCIENCES, Shanghai, China), 0.01 g NaCl (Knowles, Chengdu, China), 0.05 g $KH_2PO_4{\cdot}3H_2O$ (Knowles, Chengdu, China), 0.04 g KH_2PO_4 (Knowles, Chengdu, China), 0.01 g $MgSO_4{\cdot}7H_2O$ (Knowles, Chengdu, China), 0.007 g $CaCl_2{\cdot}2H_2O$ (Knowles, Chengdu, China), 2 g $NaHCO_3$

(Knowles, Chengdu, China), 2 mL Tween 80 (Servicebio, Wuhan, China), 0.05 g hemin (Sigma, Dorset, UK), 10 μL vitamin K1 (Haibo, Qingdao, China), 0.5 g cysteine hydrochloride, and 1 mg resazurin (Yuanye, Shanghai, China). Configuration of the basal medium took place within an anaerobic environment comprising nitrogen gas, with the pH meticulously maintained at 6.7±0.1. Firstly, anaerobic water was brought to a boil, followed by rapid cooling under running water. Subsequently, cysteine hydrochloride was added, and the air in the water was replaced with nitrogen gas (15–30 min). Other nutrients were then added, and after complete dissolution, the medium was aliquoted into anaerobic bottles. Nitrogen gas was introduced into the bottles for approximately 25 s to remove residual air. The bottles were then sealed with isobutylene stoppers and aluminum caps, and sterilized at 121°C for 15 min. Shortly after inoculation, each group of fermentation bottles received an addition of 1 mL of CDCA (MedChemExpress, New Jersey, USA) at concentrations of 10 mg mL^{-1}, 5 mg mL^{-1}, and 1 mg mL^{-1}, respectively, to the medium. In contrast, the control fermentation bottles received an additional 1 mL of culture medium. Each group consisted of three replicates. Subsequent to the initiation of fermentation, samples (1 mL) were withdrawn at specific time points (0, 6, 12, 24, 36, and 48 h) following the incubation with the bile acid substrate for the quantification of *R. lituseburensis* abundance.

2.8. Enumeration of *R. lituseburensis* by real-time quantitative PCR (qPCR)

DNA extraction from the 1 mL ileal contents culture medium was carried out using a FastPure Bacteria DNA Isolation Mini Kit (Vazyme, Nanjing, China), following the manufacturer's protocol. Subsequently, the extracted DNA was subjected to qPCR analysis on a real-time PCR instrument. To assess the abundance of specific bacterial groups, real-time qPCR was employed using the *R. lituseburensis* primer (forward: TGACATCCTTTTGACCTCTC; reverse: GCCTCACGACTTGGCTG) (Ohashi and Fujisawa 2019). The qPCR reaction mixture contained 2 μL DNA template, 0.4 μL forward primer, 0.4 μL reverse primer, 7.2 μL ddH_2O, and 10.0 μL 2×Taq Pro Universal SYBR qPCR Master Mix (Vazyme, Nanjing, China). The qPCR amplification conditions were as follows: 95°C for 30 s; 40 cycles of 95°C for 5 s and 60°C for 30 s. The standard curve was prepared according to the previous experimental procedures (Liu *et al.* 2020).

2.9. Antibiotic pretreatment and inoculation of *R. lituseburensis*

Prior to the start of the experiment, fecal samples were randomly collected from 30 individuals to assess the total bacterial count at the onset of the experiment. Before transplantation, all geese were kept on antibiotics (containing 30 mg mL^{-1} ampicillin, 30 mg mL^{-1} metronidazole, 30 mg mL^{-1} neomycin, and 15 mg mL^{-1} vancomycin) at 2 mL for 5 consecutive days to enhance engraftment efficiency of *R. lituseburensis*. Antibiotic administration was halted on the 6th day, and fecal samples were randomly collected from 30 individuals. DNA extraction from fecal samples before and after antibiotic administration was performed using the method described earlier, and qPCR experiments were conducted using primers (1369F: CGGTGAATACGTTCYCGG; 1492R: GGWTACCTTGTTACGACTT) (Suzuki *et al.* 2000) and the aforementioned method (described in Section 2.8). On the 7th day, the experimental group of geese was orally administered *R. lituseburensis* strain (Guangdong Microbial Culture Collection Center (GDMCC, No. 1.2509) at a concentration of 10^9 CFU mL^{-1} (2 mL/goose/day), while the control group received an equivalent volume of anaerobic physiological saline. The process of preparing *R. lituseburensis* suspension is briefly described as follows: First, *R. lituseburensis* was activated by incubating at 37°C in anaerobic BHI medium for 14 h. Subsequently, after passage cultivation for 14 h, the culture was centrifuged at 9,000×g for 5 min. Following centrifugation, the supernatant was carefully discarded, and PBS was added to adjust the concentration of the thawed microbiota suspension to 10^9 CFU mL^{-1}. All procedural steps, except centrifugation, were conducted within an anaerobic glovebox. Blood serum, bile acid, liver, ileum, and ovary were collected after 14 d of bacterial inoculation. The content of CDCA in serum, bile, and liver was determined using the method described in Section 2.3.

2.10. Ovary histological observation

A sliced piece of ovary tissue was taken and fixed in 10% buffered neutral formalin solution for 24 h. The fixed tissues were dehydrated in alcohol of ascending concentrations — that is, 75%, 85%, 95%, and absolute alcohol-cleared in xylene, unfiltered, and embedded in molten paraffin wax. A rotary microtome (Leica, Oskar-Barnack, Munich, Germany) was used to cut the specimens into slices of 4 μm thickness. Cross-sections were further stained with hematoxylin-eosin staining (HE) and photographed with a Pannoramic MIDI Panorama Scanner (3DHISTECH Co., Ltd., Budapest, Hungary). The panoramic scanning data were viewed in the Case Viewer software, and the number of primary and secondary follicles was counted.

2.11. Identification and validation of DEGs in the ovaries

The DEGs in the ovaries between the RI and the control group were identified using the Section 2.4 method. Meanwhile, cDNA was synthesized according to the instructions of the reverse transcription kit HiScript III RT SuperMix for qPCR (+gDNA wiper) (R323-01, Vazyme Biotechnology Co., Ltd., China). Primer 5.0 was used to design the primers (Appendix A) for key DEGs; *β-ACTIN* and *GAPDH* were used as housekeeping genes. The qPCR reaction system was as follows: 2×Taq Pro Universal SYBR qPCR Master Mix (Vazyme, Nanjing, China), 10.0 μL; PCR forward primer (10 mmol L^{-1}), 0.4 μL; PCR reverse primer (10 mmol L^{-1}), 0.4 μL; cDNA, 2 μL; ddH_2O, 7.2 μL. The qPCR amplification conditions were as follows: 95°C for 30 s; 40 cycles of 95°C for 5 s and 60°C for 30 s. The $2^{-\Delta\Delta CT}$ method was used for normalization of the qPCR results; the normalized data were then used for statistical analysis, and $P<0.05$ was considered statistically significant.

3. Result

3.1. Phenotypic identification reveals metabolic abnormalities in RD geese

The results of dissection indicate that the ovaries of the geese in the normal group display a distinct hierarchy of various follicles, whereas those in the RD group only show pre-hierarchical follicles, lacking hierarchical follicles (Fig. 2-A). Furthermore, our investigation extended to ELISA assays, affirming a noteworthy elevation in serum insulin levels within the RD group when compared to the normal group. Additionally, the serum GLU and TG levels in the RD group were significantly higher than those in the normal group. Although there was no significant difference in total CH levels between the two groups, the serum HDL-C levels were significantly higher in the RD group, while the LDL-C levels were significantly lower than those in the normal group (Fig. 2-B). At 2 wk of age, the body weight of geese in the RD group was significantly higher than that of the normal group (P<0.01), while at 43 wk of age, the body weight of geese in the RD group was significantly lower than that of the normal group (P<0.05) (Fig. 2-C). Fig. 2-D shows that while TCDCA was the predominant bile acid type in both groups of geese, substantial alterations in the metabolic profile of serum bile acids were observed between the normal and RD groups. Notably, the levels of CDCA and 7KLCA were markedly higher in the RD group compared to the normal group (Fig. 2-E).

3.2. Molecular comparison highlights the key role of bile acid metabolism in goose RD

Transcriptomic results reveal there were 150 DEGs in the ovarian stroma between the two groups, involving metabolic, fat digestion and absorption, and bile secretion pathways (Fig. 3-A). From the transcriptomic data of the liver, the DEGs are most prominently enriched in the PPAR signaling pathway, which is associated with lipid metabolism (Fig. 3-B). This pathway encompasses gene expression variations in *FABP7*, *SCD5*, *PPARG*, *APOC3*, *PLIN2*, and *Apoa2*. Notably, the bile secretion pathway was significantly enriched by the DEGs in the ileum (Fig. 3-C), and the expression levels of several genes associated with bile acid absorption (*SLC10A2/ASBT*, *SLC5A1/SGLT1*, *SLC9A3/NHE3*, *SLC51A/OSTα*, *SLC51B/OSTβ*) were found to be downregulated in the RD group. Besides, *PPARA*, *ACOX1*, *NR1H4/FXR*, *ABCG5*, *FABP1*, *HMGCR*, *ABCG8*, and *PCK1* play a central

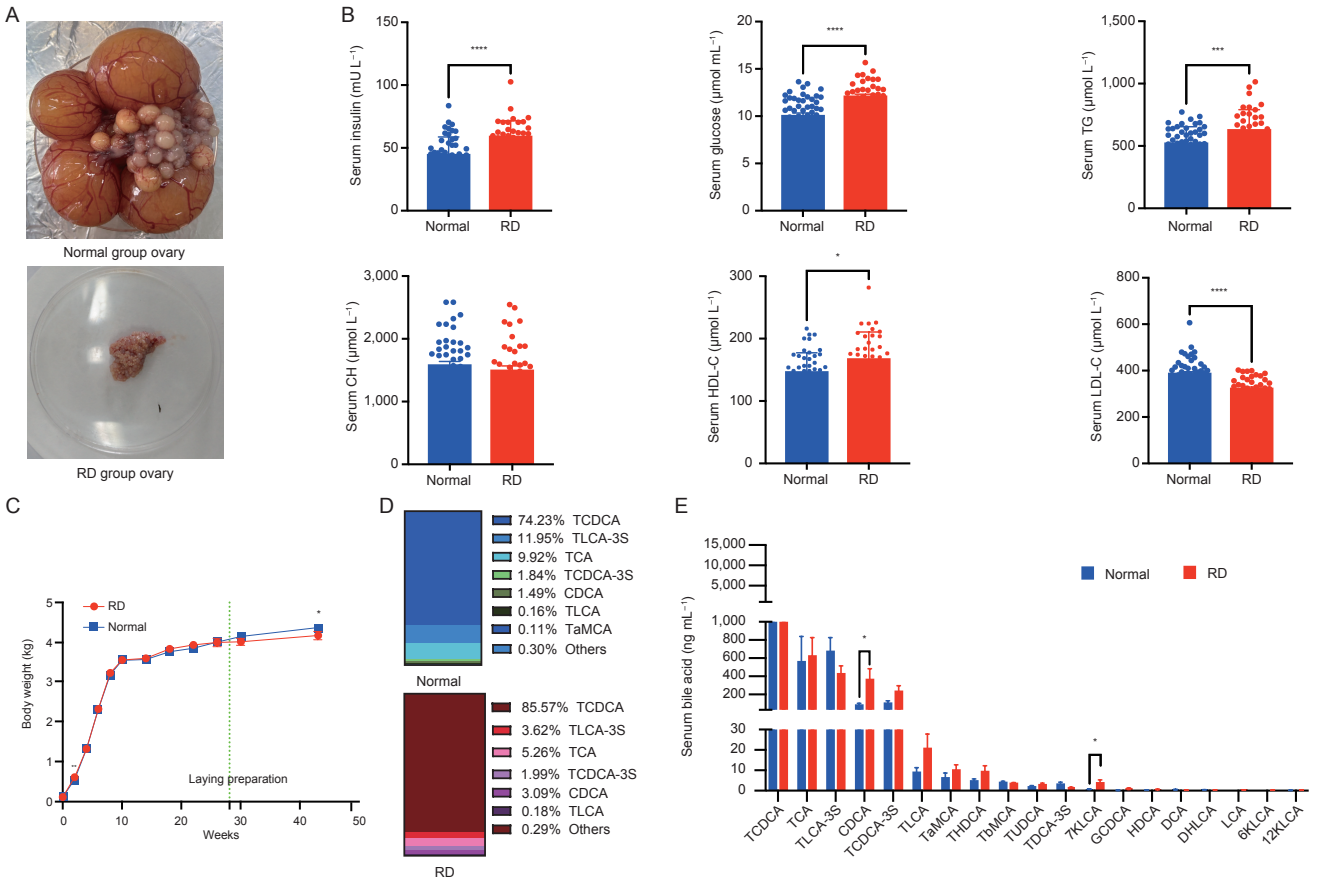


Fig. 2 Comparison of phenotypic differences between normal and reproductive disorders (RD) geese. A, comparative analysis of ovarian morphology in normal versus RD groups. B, serum lipid metabolism concentration between normal and RD groups, n=40. TG, triglycerides; CH, cholesterol; HDL-C, high-density lipoprotein cholesterol; LDC-C, low-density lipoprotein cholesterol. *, P<0.05; ***, P<0.001; ****, P<0.0001. C, the body weight of RD and normal group geese at different stages, total sample=236. *, P<0.05. D, column stacking diagram displaying serum bile acid composition between normal and RD geese (displaying bile acids with concentrations above 0.1%), n=10. E, serum untargeted metabolomic profiling to assess the bile acid levels in the serum of normal geese and RD geese, total sample=90. *, P<0.05.

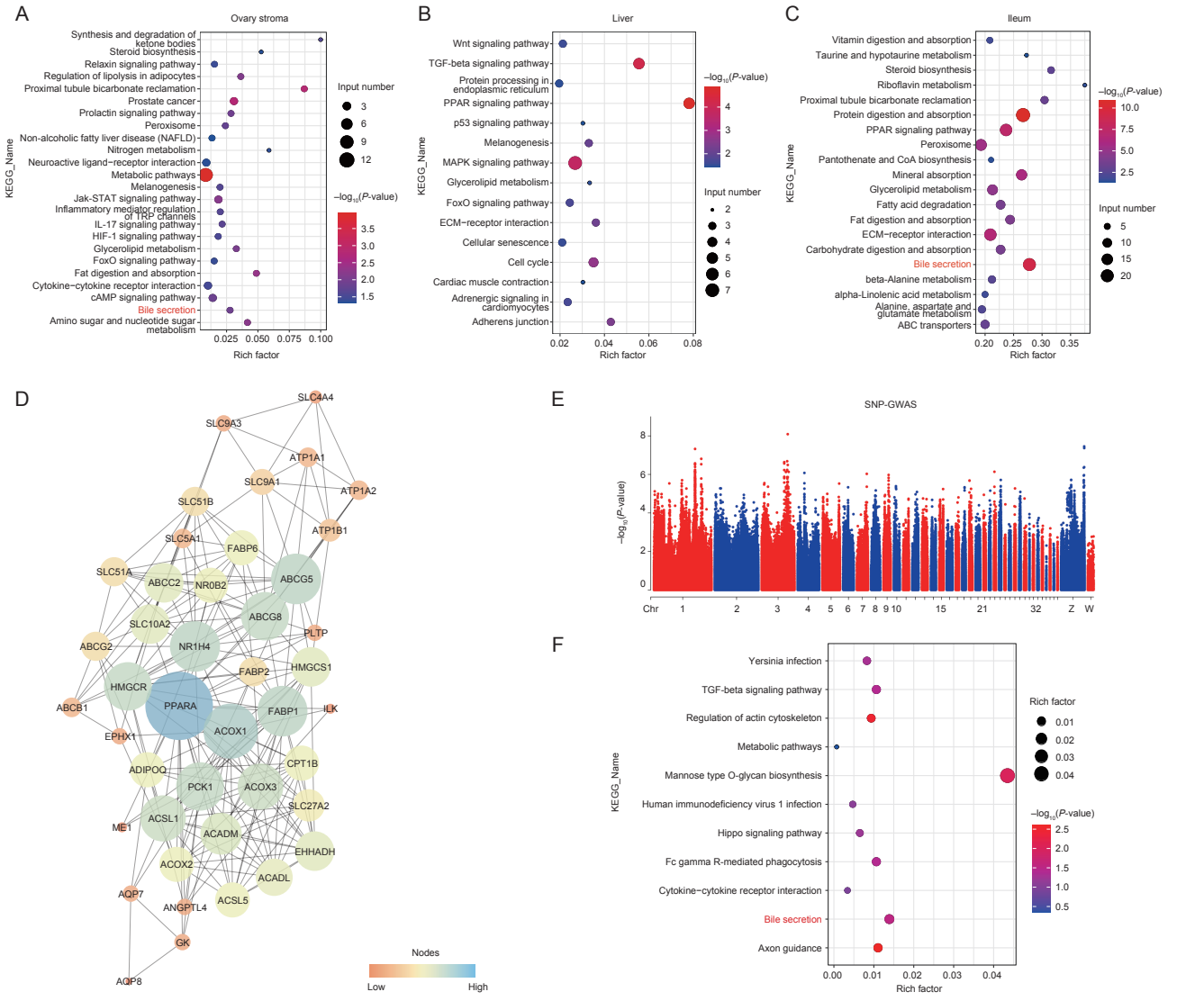


Fig. 3 Molecular mechanism analysis of geese affected by reproductive disorders (RD). A, bubble chart representation of significant KEGG pathway enrichment in ovary differentially expressed genes (DEGs) across normal and RD groups, $P<0.05$. B, bubble chart representation of significant KEGG pathway enrichment in liver DEGs across normal and RD groups, $P<0.05$. C, bubble chart representation of significant KEGG pathway enrichment in ileum DEGs across normal and RD groups, $P<0.05$. D, PPI constructed by DEGs related to lipid metabolism (including bile acid metabolism) in the ileum. E, Manhattan plot depicting GWAS results for RD in geese, $n=236$. F, bubble plot revealing significant KEGG pathways relevant to RD in geese, $P<0.05$.

role in the PPI created by DEGs related to ileal lipid and bile acid metabolism (Fig. 3-D), while only the expression of *NR1H4/FXR* was upregulated in the RD group. Appendix B demonstrates that we obtained a total of 25,212,504,941 raw reads through sequencing, with an average sequencing depth of 25.95 per individual. Additionally, we identified 12,515,997 SNPs, of which 179 were significantly associated with goose RD (Fig. 3-E), particularly involving the bile acid KEGG pathway (Fig. 3-F).

3.3. CDCA alters the microbiota in the ileum

To investigate the potential involvement of microorganisms in the RD of geese, we conducted 16S rRNA sequencing on the ileum microbiota of two groups. The results showed that although there was no significant difference in alpha diversity between the two groups (Fig. 4-A), the beta diversity in the RD group was significantly higher than that of the normal group (Fig. 4-B). As shown in Fig. 4-C, the RD and normal groups have 632 and 420 specific ASVs and 262 core ASVs. The stacked bar chart displays the composition of different samples at genus level, with *Lactobacillus* having the highest abundance in all samples (Fig. 4-D). Both random forest analysis (Fig. 4-E) and LEfSe analysis (Fig. 4-F) showed significant differences in the *Romboutsia* abundance between the RD group and the normal group. To further validate these findings, *in vitro* ileum content cultivation and bile acid supplementation experiments were conducted, confirming the stimulatory effect of CDCA on the abundance of *R. lituseburensis*, exhibiting a dose-dependent response (Fig. 4-G). Specifically, compared to the group without added CDCA, the addition of CDCA at a concentration of 5 mg mL^{-1} did not alter the abundance of *R. lituseburensis*. However,

the addition of CDCA at a concentration of 1 mg mL^{-1} significantly increased the abundance of *R. lituseburensis* at both 24 and 48 h. Furthermore, when CDCA was added at a concentration of 10 mg mL^{-1}, there was a significant increase in the abundance of *R. lituseburensis* at 24 and 36 h.

3.4. *Romboutsia lituseburensis* modulates lipid metabolism and immunity while inhibiting in goose follicle development

As shown in Fig. 5-A, our results indicate a significant increase in the abundance of *Romboutsia* in both the cecum and ileum after gavage with *R. lituseburensis*, compared to the control group. However, there was no significant change in the CDCA concentration between the *R. lituseburensis* group (RI) and the control group in serum, bile, or liver (Appendix C). The number of primary follicles in the ovaries of the RI group was significantly lower than that of the control group (Fig. 5-B). Meanwhile, the content of CH and HDL-C in the serum of the RI was significantly higher than that of the control group, while the content of IgA, IgG, IgM, and LPS was significantly

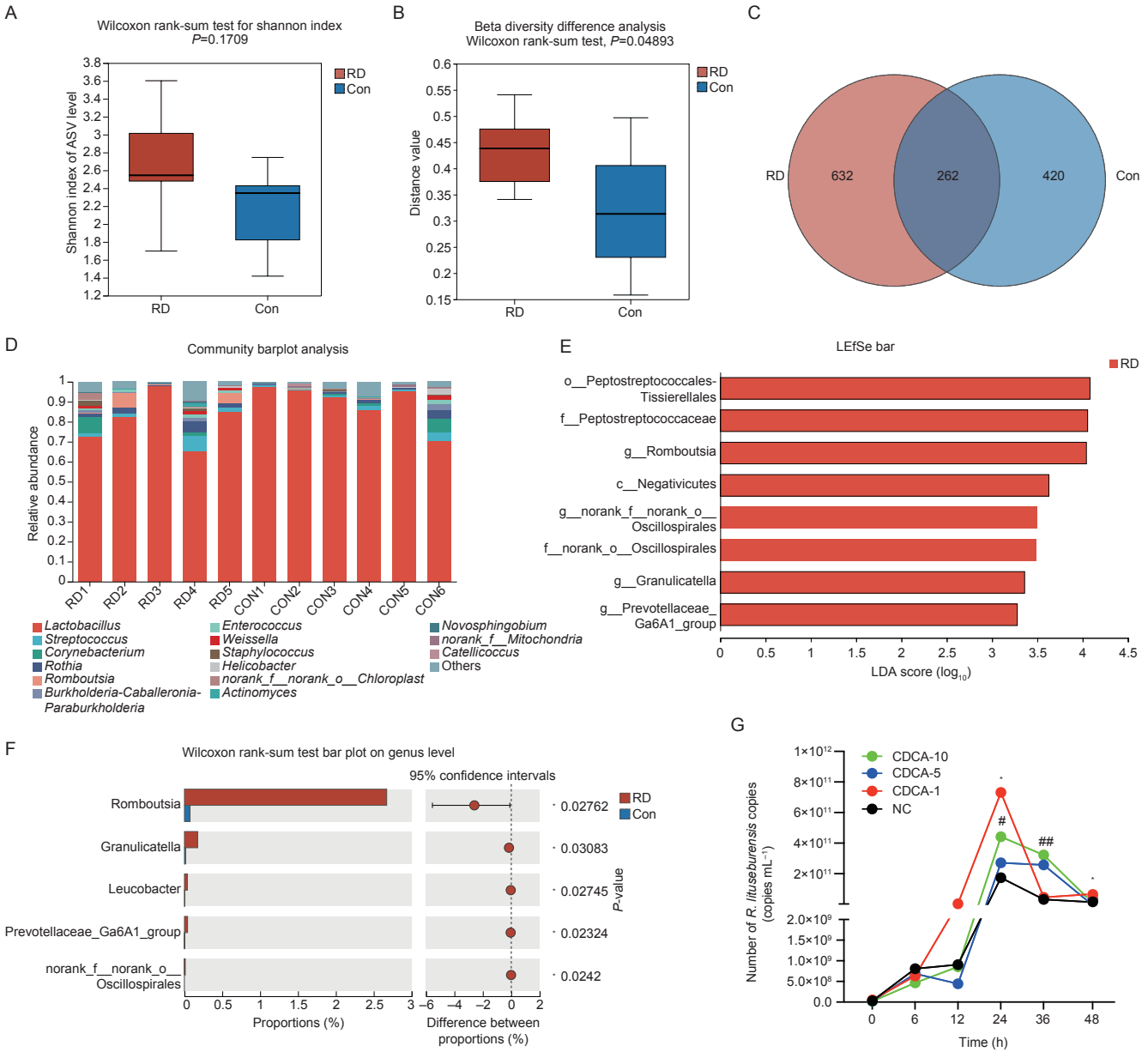


Fig. 4 Microbial insights and chenodeoxycholic acid (CDCA) promotion in geese gut microbiota. A, the box plots show the Shannon diversity index of reproductive disorders (RD) and normal groups. B, the box plots show the beta diversity index of RD and normal groups. C, the Venn diagram shows unique and core ASVs between RD and normal groups. D, histograms of the relative abundances of the top bacterial communities at genus level of all samples. E, LEfSe analysis identifies biomarkers for the microbiota in the ileum of the RD group. F, investigation of differential microbial abundance between the RD and normal groups was conducted through an inter-group difference significance test using the Wilcoxon rank-sum test (P<0.05). G, the schematic diagram illustrates the *in vitro* cultivation experiment of ileal contents and the supplementary impact of CDCA on the number of *Romboutsia lituseburensis*, n=4. *, P<0.05 for CDCA-1 *vs.* NC; $^{\#}$, P<0.05 for CDCA-10 *vs.* NC; $^{\#\#}$, P 0.01 for CDCA-10 *vs.* NC.

lower than that of the control group (Fig. 5-C). The serum CH content is significantly positively correlated with LDL-C, HDL-C, GLU, and TG, while it is significantly negatively correlated with IgA, IgM, and LPS (Fig. 5-D). After gavage with *R. lituseburensis*, the expression levels of genes related to oocyte meiosis and maturation (*CPEB4*, *ITPR2*, *ITPR3*, *PDE3B*, *ADCY9*, and *BRAF*) in the ovaries were significantly downregulated (Fig. 5-E). The DEGs in the ovaries between the two groups were most significantly enriched in pathways related to immune-associated chemokines signaling and cytokine–cytokine receptor interactions (Table 1). *CCL4*, *CCR4*, *CCR7*, *CXCR1*, *FAK2*, *JAK2*, *PLCB2*, *LYN*, *PREX1*, *RAC2*, and *NCF1*, involved in the chemokines signaling pathway, are significantly downregulated in the RI (Fig. 5-F). Meanwhile, *CD3E*, *CD4*, *CSF1R*, *CSF2R*, *IL16*, and *IL18*, involved in the cytokine-cytokine receptor interactions pathway, are significantly downregulated in the RI group (Fig. 5-G). Additionally, Fig. 5 demonstrates the consistency between the transcriptomic and qPCR results.

4. Discussion

Our findings suggest that geese with RD lack hierarchical

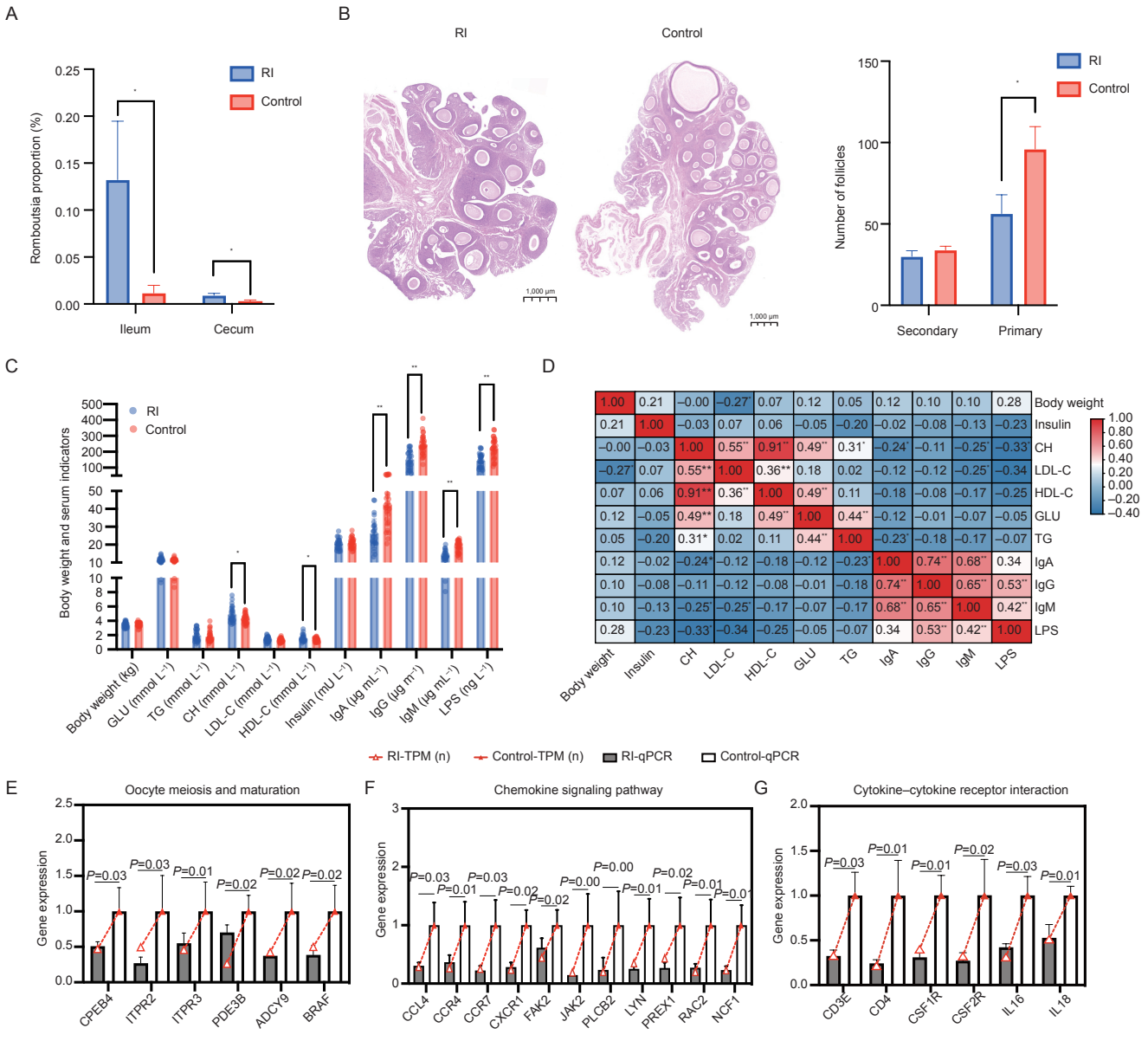


Fig. 5 Phenotypic and molecular evidence in the effect of gavage with *Romboutsia lituseburensis* on reproduction in geese. A, differences in the abundance of *Romboutsia* between *R. lituseburensis* group (RI) and control group, n=10. *, P<0.05. B, differences in the ovary morphology and number of follicles between RI and control groups, n=6. C, the body weight and serum biochemical indicators between the RI and control groups, n=30. GLU, serum glucose; TG, triglycerides; CH, cholesterol; HDL-C, high-density lipoprotein cholesterol; LDC-C, low-density lipoprotein cholesterol. *, P<0.05; **, P<0.01. D, heat map of correlation analysis between serum biochemical indicators. E, representative differentially expressed genes (DEGs) expression levels in the oocyte meiosis and maturation pathway, n=4. F, representative DEGs expression levels in the chemokines signaling pathway, n=4. G, representative DEGs expression levels in the cytokine–cytokine receptor interaction pathway, n=4.

Table 1 The KEGG pathway significantly enriched with differentially expressed genes (DEGs) in the ovaries between *Romboutsia lituseburensis* group (RI) and control group

KEGG_name	Input DEGs	*P*
Cytokine–cytokine receptor interaction	*INHA*, *IL18*, *TGFB3*, *CCL4*, *IL2RG*, *CSF1R*, *IL16*, *CD4*, *CXCR1*, *CCR4*, *CXCR5*, *CCR7*, *GDF11*	0.00
Calcium signaling pathway	*CD38*, *PLCB2*, *ADRB1*, *ADCY9*, *PLCG2*, *GNA14*, *ITPR2*, *ITPR3*, *P2RX3*	0.00
Apelin signaling pathway	*PLCB2*, *SMAD4*, *ADCY9*, *PDE3B*, *ITPR2*, *ITPR3*, *PLIN1*	0.00
Chemokine signaling pathway	*PLCB2*, *IPMK*, *PLCG2*, *ITPR2*, *ITPR3*, *MTMR3*	0.00
ABC transporters	*ABCA9*, *TAP2*, *ABCA5*, *ABCA1*	0.00
Vascular smooth muscle contraction	*PLCB2*, *ADCY9*, *BRAF*, *ITPR2*, *ITPR3*, *CALD1*	0.00
Gap junction	*ITPR2*, *ITPR3*, *PLCB2*, *ADCY9*, *ADRB1*	0.01
FoxO signaling pathway	*TGFB3*, *RBL2*, *SMAD4*, *G6PC*, *S1PR4*, *BRAF*	0.01
NOD-like receptor signaling pathway	*IL18*, *PLCB2*, *TRAF5*, *CASP8*, *ITPR2*, *ITPR3*	0.01
C-type lectin receptor signaling pathway	*ITPR2*, *PLCG2*, *IRF1*, *CASP8*, *ITPR3*	0.01
Lysine degradation	*KMT2C*, *KMT2A*, *ASH1L*, *KMT2E*	0.01
Adrenergic signaling in cardiomyocytes	*PLCB2*, *CREB5*, *ADCY9*, *TPM1*, *TPM2*, *ADRB1*	0.01
TGF-beta signaling pathway	*SMAD4*, *GREM1*, *ID4*, *TGFB3*, *FMOD*	0.01
AGE-RAGE signaling pathway in diabetic complications	*SMAD4*, *PLCG2*, *PLCB2*, *TGFB3*, *JAK2*	0.01
Salmonella infection	*IL18*, *FLNC*, *RHOG*, *CCL4*	0.01
Inositol phosphate metabolism	*PLCG2*, *PLCB2*, *IPMK*, *MTMR3*	0.01
Progesterone-mediated oocyte maturation	*CPEB4*, *PDE3B*, *ADCY9*, *BRAF*	0.02
GnRH signaling pathway	*ITPR2*, *ITPR3*, *PLCB2*, *ADCY9*	0.02
Glutathione metabolism	*GGT1*, *GSTT1*, *GPX2*	0.02
Apoptosis	*ITPR2*, *CFLAR*, *ERN1*, *CASP8*, *ITPR3*	0.02
Arachidonic acid metabolism	*LTC4S*, *GGT1*, *GPX2*	0.03
Necroptosis	*CFLAR*, *JAK2*, *JAK3*, *CASP8*, *TRAF5*	0.03
Neuroactive ligand-receptor interaction	*GRIK1*, *S1PR4*, *ADRB1*, *P2RY8*, *C5AR1*, *HRH3*, *LPAR2*, *P2RX3*, *P2RY1*	0.03
Regulation of actin cytoskeleton	*RAC2*, *ABI2*, *LIMK1*, *BRAF*, *LPAR2*, *LPAR5*	0.04
Cellular senescence	*ITPR2*, *ITPR3*, *HIPK1*, *TGFB3*, *RBL2*	0.04
Oocyte meiosis	*ITPR2*, *CPEB4*, *ADCY9*, *ITPR3*	0.04
Herpes simplex virus 1 infection	*SRSF5*, *TAP2*, *JAK2*, *TRAF5*, *CASP8*	0.04

follicles. Additionally, noteworthy distinctions were observed in the lipid metabolism functionality of RD geese compared to the normal group. Previous research has suggested that these observations align with the phenotypes of follicular developmental disorders seen in mammalian PCOS, ovarian dysfunction, or ovarian inflammation (Boots and Jungheim 2015; Kumariya *et al.* 2021). Moreover, lipid metabolism plays a crucial role in oocyte and granulosa cell development, serving as both an energy source and substrate for various intracellular processes (Wu *et al.* 2010; Dunning *et al.* 2014; Wang *et al.* 2015). Interestingly, in RD geese, both insulin and glucose levels were found to be elevated in the serum, coupled with a decrease in body weight. This may indicate the occurrence of insulin resistance, potentially induced by abnormalities in lipid metabolism.

In recent years, it has been confirmed that abnormalities in lipid metabolism can lead to infertility and various RD. Consequently, abnormalities in lipid metabolism can lead to infertility and various RD, such as PCOS (Wild *et al.* 2011; Lai *et al.* 2014), ovarian cancer (Tania *et al.* 2010), and preeclampsia (De Lima *et al.* 2011). Among women with PCOS, the estimated prevalence of obesity ranges from 30 to 70%, establishing a link among obesity (Barber *et al.* 2006), inflammation, and insulin resistance (Diamanti-Kandarakis and Dunaif 2012). Lipid abnormalities in women with PCOS encompass altered levels of LDL-C, TG, and HDL-C, along with changes in lipid species (Jové *et al.* 2018), resulting in a prevalence of lipid abnormalities among these patients ranging from 50 to 60% (Wild *et al.* 2011). Our transcriptome results in the liver and ileum seem to confirm the cause of this serum lipid change. *PPARG* regulates the storage of fatty acids and lipoprotein metabolism, and its upregulation in the liver may promote adipocyte differentiation and lipid storage, potentially contributing to an increase in TG levels (Ahmadian *et al.* 2013). Additionally, *SCD5* is involved in the production of unsaturated fatty acids, which can affect the assembly and secretion of lipoproteins, thereby influencing TG levels (Igal and Sinner 2021). *APOA2* is a major component of HDL-C, and its downregulation may be associated with changes in HDL-C function (Welch *et al.* 2004). However, the increase in HDL-C levels suggests the involvement of other mechanisms in regulating HDL-C synthesis or clearance. For example, *LIPG*, which primarily acts on HDL-C phospholipids, may also affect HDL-C metabolism and circulation (Jaye and Krawiec 2004). Its upregulation may also be related to the increase in HDL-C levels. Furthermore, the significant changes in the expression levels of multiple genes related to cholesterol metabolism (*HMGCR* (Sharpe and Brown 2013), *ABCG5*, and *ABCG8* (Yu *et al.* 2014)) in the ileum may also be associated with changes in serum HDL-C and LDL-C levels. Together, these results support the notion that when geese experience RD, their bodies manifest lipid metabolism disorders.

This phenomenon prompted us to investigate the potential genetic and metabolic factors underlying it. GWAS have proven instrumental in unraveling genetic mechanisms across various traits in poultry (He *et al.* 2023). Our GWAS

results point to specific metabolic pathways, notably bile acid metabolism, as being associated with RD in geese. Additionally, our findings have indicated that geese with RD exhibited significantly higher serum levels of CDCA and 7KLCA compared to the normal group. Furthermore, these results represent the first demonstration of the composition of bile acids in goose serum. Unlike mice and humans (Rees *et al.* 2017; Zheng *et al.* 2021), TCDC is the most abundant bile acid in goose serum, which might be attributed to certain unique avian physiological characteristics. Interestingly, we have observed a significant downregulation of multiple genes associated with bile acid absorption, including *SLC10A2/ASBT* (Xiao and Pan 2017), *SLC5A1/SGLT1*, *SLC9A3/NHE3*, *SLC51A/OSTα*, and *SLC51B/OSTβ* (Ballatori *et al.* 2013) in the ileum. Concurrently, the expression levels of genes related to bile acid synthesis remain unchanged in the liver, proving that impaired absorption of bile acids may lead to changes in serum bile acid composition (Lan *et al.* 2011). *NR1H4*/*FXR* is a nuclear receptor involved in the regulation of bile acids. The upregulation of *NR1H4*/*FXR* may be a compensatory response of the body to a decrease in bile acid absorption. It has been proven in the literature that the activation of *NR1H4*/*FXR* can regulate bile acid synthesis and metabolism, thereby affecting the content of bile acids (Lambert *et al.* 2003). *NR1H4*/FXR is an effective activator of CDCA (Tu *et al.* 2000), which may be closely related to the observed upregulation of CDCA content in serum. Bile acids can also play a role in lipid metabolism through pathways such as *NR1H4*/*FXR*, thereby influencing the levels of cholesterol, insulin, and glucose (Lundasen *et al.* 2012). These findings strongly indicate that changes in serum lipid metabolism may be associated with genetically induced bile acid absorption disorders.

Bile acids can interact with gut microbiota, regulating the balance of gut microbiota types and microbiota (Clements *et al.* 1996; Lorenzo-Zuniga *et al.* 2003; Devkota *et al.* 2012). Our research findings indicate a significant increase in the abundance of *Romboutsia* in the ileum microbiota of geese with RD. The relative abundance of *Romboutsia* is associated with fat accumulation, and moderate-intensity exercise has been shown to alter the relative abundance of *Romboutsia* (Yin *et al.* 2022). *Romboutsia* decreases after completing a half-marathon race, while a high-fat diet increases the relative abundance of *Romboutsia* (Zhang *et al.* 2020). An increase in the abundance of *Romboutsia* has been observed in obese and diabetic populations (Zeng *et al.* 2019; Therdtatha *et al.* 2021; Vazquez-Moreno *et al.* 2021; Zhou *et al.* 2021), and dietary regulation has been proven to reduce the abundance of *Romboutsia* bacteria while simultaneously improving phenotypes (Lei *et al.* 2023). In previous studies, the addition of heterologous bile salts could isolate *Romboutsia* (Gerritsen *et al.* 2014), and our results also demonstrate that CDCA promotes the abundance of *Romboutsia*.

Research has indicated a negative correlation between the abundance of *Romboutsia* in the vagina (Wen *et al.* 2021) and intestines (Yang *et al.* 2020; Han *et al.* 2022) and the reproductive performance of poultry. *R. lituseburensis* has been isolated in the chicken intestine (Liu *et al.* 2023a), indicating its dominance in the poultry intestine. Our study, for the first time, confirmed the impact of gavage with *R. lituseburensis* on its mechanism. Our findings revealed that *R. lituseburensis* significantly reduced the number of primary follicles in goose ovaries and downregulated the expression levels of several genes associated with oocyte meiosis and maturation, including *CPEB4* (Igea and Méndez 2010), *ITPR2*, *ITPR3* (Vicente *et al.* 2022), *PDE3B* (Tsafriri *et al.* 1996), *ADCY9*, and *BRAF* (Guida *et al.* 2022). These results indicate that *R. lituseburensis* inhibits the occurrence of primary follicles through the molecular pathway of oocyte meiosis and maturation, potentially leading to RD in geese. Furthermore, gavage with *R. lituseburensis* also altered the immune profiles of geese, including IgA, IgM, and IgG, consistent with previous experiments (Mignot *et al.* 1989; Liu *et al.* 2023b). Significant changes were observed in immune-related pathways within the ovaries following *R. lituseburensis* gavage, including chemokine and cytokine-cytokine receptor interaction pathways. Since 1980, researchers have proposed that the immune system can regulate ovulation and ovarian function (Bukovsky and Presl 1979). It has been established that ovulation is an inflammatory response, and necessary inflammation is crucial for ovulation initiation (Duffy *et al.* 2019). The roles of chemokines and cytokines as important immune regulatory factors in reproductive defects have been repeatedly emphasized. Although IL-18 is used as a biomarker for PCOS in humans (Ebejer and Calleja-Agius 2013), our results show lower *IL-18* expression in the ovaries of the RI, suggesting a potential immune mechanism distinct from mammalian ovarian function. For example, our results indicate a significant downregulation of *IL-16* and its receptor *CD4* in the RI ovaries, which have been shown to function in primordial follicular development (Feeney *et al.* 2014). These results support the involvement of *R. lituseburensis* in reducing the number of primary follicles through immune factor-mediated follicular development.

5. Conclusion

In summary, our comprehensive study elucidates the complexity of RD in geese, offering a multifaceted perspective that spans phenotypic and molecular analyses between normal and RD-affected individuals. Our genomic analysis identified mutations in genes associated with bile acid metabolism, pinpointing them as potential contributors to RD in geese. This discovery is supported by targeted bile acid metabolome and ileum transcriptome data, which demonstrate impaired bile acid absorption in the ileum, *FXR* activation, and elevated serum CDCA levels in RD-affected geese. Additionally, our exploration of the ileal microbiota revealed the significant role of microbial communities, particularly *Romboutsia*, in the regulation of RD in geese. *In vitro* cultivation experiments of ileal contents provided compelling evidence that CDCA promotes the growth of *R. lituseburensis*. Further, gavage of *R. lituseburensis* in geese resulted in a reduction of primary follicles in the ovaries, likely due to *R. lituseburensis* mediating a slowdown in follicular development through the downregulation of immune factors. Our findings not only deepen our understanding of the etiology of RD in geese but also

suggest potential therapeutic interventions targeting bile acid metabolism and the modulation of specific microbiota components. This research offers new insights into the interaction between host phenotype and gut microbiota and may have broader implications in the fields of avian biology and reproductive medicine.

Acknowledgements

This research was supported by China Agriculture Research System of MOF and MARA (CARS-42-4) and Key Technology Support Program of Sichuan Province, China (2021YFYZ0014) for the financial support. I would like to express my gratitude to Professor Min Hu and Professor Honggang Yin from Guangzhou Sport University for their assistance in providing the *R. lituseburensis*.

Declaration of competing interest

The authors declare that they have no conflict of interest.

Declaration of generative AI and AI-assisted technologies in the writing process

The authors declare that they did not use AI in the preparation and writing of this manuscript.

Ethical approval

The present research was conducted in accordance with the rules for the care of laboratory animals (2017 Revision) formulated by the State Council of China, and the protocol was approved by the Animal Care and Use Committee of Sichuan Agricultural University, Chengdu, China (approval no. 20201005). All animal experiments were carried out in accordance with the ARRIVE guidelines.

Data availability

The sequencing data generate in this study is available in the NCBI. The accession number of 16S RNA gene sequencing data is PRJNA1061353. The accession number of transcriptome data is PRJNA1061459 (ileum), PRJNA1061654 (ovary stroma), PRJNA1061681 (liver) and PRJNA1061807 (ovary).

Appendices associated with this paper are available at https://doi.org/10.1016/j.jia.2024.05.030

References

Ahmadian M, Suh J M, Hah N, Liddle C, Atkins A R, Downes M, Evans R M. 2013. PPARγ signaling and metabolism: The good, the bad and the future. *Nature Medicine*, **19**, 557–566.

Ballatori N, Christian W V, Wheeler S G, Hammond C L. 2013. The heteromeric organic solute transporter, OSTα-OSTβ/SLC51: A transporter for steroid-derived molecules. *Molecular Aspects of Medicine*, **34**, 683–692.

Barber T M, McCarthy M I, Wass J A, Franks S. 2006. Obesity and polycystic ovary syndrome. *Clinical Endocrinology*, **65**, 137–145.

Bolyen E, Rideout J R, Dillon M R, Bokulich N A, Abnet C C, Al-Ghalith G A, Alexander H, Alm E J, Arumugam M, Asnicar F, Bai Y, Bisanz J E, Bittinger K, Brejnrod A, Brislawn C J, Brown C T, Callahan B J, Caraballo-Rodriguez A M, Chase J, Cope E K, *et al.* 2019. Author correction: Reproducible, interactive, scalable and extensible microbiome data science using QIIME 2. *Nature Biotechnology*, **37**, 1091.

Boots C E, Jungheim E S. 2015. Inflammation and human ovarian follicular dynamics. *Seminars in Reproductive Medicine*, **33**, 270–275.

Broughton D E, Moley K H. 2017. Obesity and female infertility: Potential mediators of obesity's impact. *Fertility and Sterility*, **107**, 840–847.

Bu D, Luo H, Huo P, Wang Z, Zhang S, He Z, Wu Y, Zhao L, Liu J, Guo J, Fang S, Cao W, Yi L, Zhao Y, Kong L. 2021. KOBAS-i: Intelligent prioritization and exploratory visualization of biological functions for gene enrichment analysis. *Nucleic Acids Research*, **49**, W317–W325.

Bukovsky A, Presl J. 1979. Ovarian function and the immune system. *Medical Hypotheses*, **5**, 415–436.

Chen X Y, Yu T T, Dou Y H, Ji Q Y, Guo L P, Geng Z Y. 2023. High dietary energy decreased reproductive performance through increasing lipid deposition in Yangzhou geese at late laying stage. *Poultry Science*, **102**, 102915.

Clements W D, Parks R, Erwin P, Halliday M I, Barr J, Rowlands B J. 1996. Role of the gut in the pathophysiology of extrahepatic biliary obstruction. *Gut*, **39**, 587–593.

Collins S L, Stine J G, Bisanz J E, Okafor C D, Patterson A D. 2023. Bile acids and the gut microbiota: Metabolic interactions and impacts on disease. *Nature Reviews Microbiology*, **21**, 236–247.

De Lima V J, De Andrade C R, Ruschi G E, Sass N. 2011. Serum lipid levels in pregnancies complicated by preeclampsia. *Sao Paulo Medical Journal*, **129**, 73–76.

Devkota S, Wang Y, Musch M W, Leone V, Fehlner-Peach H, Nadimpalli A, Antonopoulos D A, Jabri B, Chang E B. 2012. Dietary-fat-induced taurocholic acid promotes pathobiont expansion and colitis in $Il10^{-/-}$ mice. *Nature*, **487**, 104–108.

Diamanti-Kandarakis E, Dunaif A. 2012. Insulin resistance and the polycystic ovary syndrome revisited: An update on mechanisms and implications. *Endocrine Reviews*, **33**, 981–1030.

Duffy D M, Ko C, Jo M, Brannstrom M, Curry T E. 2019. Ovulation: Parallels with inflammatory processes. *Endocrine Reviews*, **40**, 369–416.

Dunaif A. 1997. Insulin resistance and the polycystic ovary syndrome: Mechanism and implications for pathogenesis. *Endocrine Reviews*, **18**, 774–800.

Dunning K R, Anastasi M R, Zhang V J, Russell D L, Robker R L. 2014. Regulation of fatty acid oxidation in mouse cumulus-oocyte complexes during maturation and modulation by PPAR agonists. *PLoS ONE*, **9**, e87327.

Ebejer K, Calleja-Agius J. 2013. The role of cytokines in polycystic ovarian syndrome. *Gynecological Endocrinology*, **29**, 536–540.

Feeney A, Nilsson E, Skinner M K. 2014. Cytokine (IL16) and tyrphostin actions on ovarian primordial follicle development. *Reproduction*, **148**, 321–331.

Gerritsen J, Fuentes S, Grievink W, van Niftrik L, Tindall B J, Timmerman H M, Rijkers G T, Smidt H. 2014. Characterization of *Romboutsia ilealis* gen. nov., sp. nov., isolated from the gastro-intestinal tract of a rat, and proposal for the reclassification of five closely related members of the genus *Clostridium* into the genera *Romboutsia* gen. nov., *Intestinibacter* gen. nov., *Terrisporobacter* gen. nov. and *Asaccharospora* gen. nov. *International Journal of Systematic and Evolutionary Microbiology*, **64**, 1600–1616.

Guida E, Tassinari V, Colopi A, Todaro F, Cesarini V, Jannini B, Pellegrini M, Botti F, Rossi G, Rossi P, Jannini E A, Dolci S. 2022. MAPK activation drives male and female mouse teratocarcinomas from late primordial germ cells. *Journal of Cell Science*, **135**, jcs259375.

Han H, Sun Y, Fan Y, Zhang H, Yang J, Chi R, Gao Y, Liu J, Li K, Li W, Liu Y. 2022. Microbial diversity and community composition of duodenum microbiota of high and low egg-yielding Taihang chickens identified using 16S rRNA amplicon sequencing. *Life*, **12**, 1262.

He Z, Liu R, Wang M, Wang Q, Zheng J, Ding J, Wen J, Fahey A G, Zhao G. 2023. Combined effect of microbially derived cecal SCFA and host genetics on feed efficiency in broiler chickens. *Microbiome*, **11**, 198.

Hermier D, Saadoun A, Salichon M R, Sellier N, Rousselot-Paillet D, Chapman M J. 1991. Plasma lipoproteins and liver lipids in two breeds of geese with different susceptibility to hepatic steatosis: Changes induced by development and force-feeding. *Lipids*, **26**, 331–339.

Herrera E, Ortega-Senovilla H. 2010. Maternal lipid metabolism during normal pregnancy and its implications to fetal development. *Clinical Lipidology*, **5**, 899–911.
Igal R A, Sinner D I. 2021. Stearoyl-CoA desaturase 5 (SCD5), a Δ-9 fatty acyl desaturase in search of a function. *Biochimica Et Biophysica Acta-Molecular and Cell Biology of Lipids*, **1866**, 158840.
Igea A, Méndez R. 2010. Meiosis requires a translational positive loop where CPEB1 ensues its replacement by CPEB4. *Embo Journal*, **29**, 2182–2193.
Jaye M, Krawiec J. 2004. Endothelial lipase and HDL metabolism. *Current Opinion in Lipidology*, **15**, 183–189.
Jové M, Pradas I, Naudí A, Rovira-Llopis S, Bañuls C, Rocha M, Portero-Otin M, Hernández-Mijares A, Victor V M, Pamplona R. 2018. Lipidomics reveals altered biosynthetic pathways of glycerophospholipids and cell signaling as biomarkers of the polycystic ovary syndrome. *Oncotarget*, **9**, 4522–4536.
Kim D, Langmead B, Salzberg S L. 2015. HISAT: A fast spliced aligner with low memory requirements. *Nature Methods*, **12**, 357–360.
Kumariya S, Ubba V, Jha R K, Gayen J R. 2021. Autophagy in ovary and polycystic ovary syndrome: Role, dispute and future perspective. *Autophagy*, **17**, 2706–2732.
Lai H, Jia X, Yu Q X, Zhang C L, Qiao J, Guan Y F, Kang J H. 2014. High-fat diet induces significant metabolic disorders in a mouse model of polycystic ovary syndrome. *Biology of Reproduction*, **91**, 127.
Lambert G, Amar M J A, Guo G, Brewer H B, Gonzalez F J, Sinal C J. 2003. The farnesoid X-receptor is an essential regulator of cholesterol homeostasis. *Journal of Biological Chemistry*, **278**, 2563–2570.
Lan T, Haywood J, Rao A, Dawson P A. 2011. Molecular mechanisms of altered bile acid homeostasis in organic solute transporter-alpha knockout mice. *Digestive Diseases*, **29**, 18–22.
Lei S, He S, Li X, Zheng B, Zhang Y, Zeng H. 2023. Effect of lotus seed resistant starch on small intestinal flora and bile acids in hyperlipidemic rats. *Food Chemistry*, **404**, 134599.
Li A, Li F, Song W, Lei Z L, Sha Q Q, Liu S Y, Zhou C Y, Zhang X, Li X Z, Schatten H, Zhang T, Sun Q Y, Ou X H. 2023. Gut microbiota-bile acid-vitamin D axis plays an important role in determining oocyte quality and embryonic development. *Clinical and Translational Medicine*, **13**, e1236.
Li H. 2013. Aligning sequence reads, clone sequences and assembly contigs with BWA-MEM. *arXiV*, 1303.3997.
Li H, Handsaker B, Wysoker A, Fennell T, Ruan J, Homer N, Marth G, Abecasis G, Durbin R, Proc G P D. 2009. The sequence alignment/map format and SAMtools. *Bioinformatics*, **25**, 2078–2079.
Liao Y, Smyth G K, Shi W. 2014. featureCounts: An efficient general purpose program for assigning sequence reads to genomic features. *Bioinformatics*, **30**, 923–930.
Liu H B, Lv Q Q, Dai L. 2020. Quantitative analysis of 16S rRNA gene copies in mouse fecal sample. *Bio-101* e2003368. doi: 10.21769/BioProtoc.2003368. (in Chinese)
Liu Y, Feng Y, Yang X, Lv Z, Li P, Zhang M, Wei F, Jin X, Hu Y, Guo Y, Liu D. 2023a. Mining chicken ileal microbiota for immunomodulatory microorganisms. *ISME Journal*, **17**, 758–774.
Liu Y, Feng Y Q, Yang X Y, Lv Z T, Li P, Zhang M H, Wei F X, Jin X L, Hu Y F, Guo Y M, Liu D. 2023b. Mining chicken ileal microbiota for immunomodulatory microorganisms. *ISME Journal*, **17**, 758–774.
Lorenzo-Zuniga V, Bartoli R, Planas R, Hofmann A F, Vinado B, Hagey L R, Hernandez J M, Mane J, Alvarez M A, Ausina V, Gassull M A. 2003. Oral bile acids reduce bacterial overgrowth, bacterial translocation, and endotoxemia in cirrhotic rats. *Hepatology*, **37**, 551–557.
Lundasen T, Andersson E M, Snaith M, Lindmark H, Lundberg J, Ostlund-Lindqvist A M, Angelin B, Rudling M. 2012. Inhibition of intestinal bile acid transporter Slc10a2 improves triglyceride metabolism and normalizes elevated plasma glucose levels in mice. *PLoS ONE*, **7**, e37787.
Martin G, Kolida S, Marchesi J R, Want E, Sidaway J E, Swann J R. 2018. *In vitro* modeling of bile acid processing by the human fecal microbiota. *Frontiers in Microbiology*, **9**, 1153.
Mignot M H, Drexhage H A, Kleingeld M, Van de Plassche-Boers E M, Rao B R, Schoemaker J. 1989. Premature ovarian failure. II: Considerations of cellular immunity defects. *European Journal of Obstetrics*, *Gynecology*, *and Reproductive Biology*, **30**, 67–72.
Ohashi Y, Fujisawa T. 2019. Analysis of cluster XI bacteria in human feces. *Bioscience of Microbiota Food and Health*, **38**, 65–68.
Ouyang Q, Hu S, Tang B, Hu B, Hu J, He H, Li L, Wang J. 2022. Comparative transcriptome analysis provides novel insights into the effect of lipid metabolism on laying of geese. *Animals*, **12**, 1775.
Patel R K, Jain M. 2012. NGS QC Toolkit: A toolkit for quality control of next generation sequencing data. *PLoS ONE*, **7**, e30619.
Qi X, Yun C, Sun L, Xia J, Wu Q, Wang Y, Wang L, Zhang Y, Liang X, Wang L, Gonzalez F J, Patterson A D, Liu H, Mu L, Zhou Z, Zhao Y, Li R, Liu P, Zhong C, Pang Y, *et al.* 2019. Gut microbiota-bile acid-interleukin-22 axis orchestrates polycystic ovary syndrome. *Nature Medicine*, **25**, 1225–1233.
Quast C, Pruesse E, Yilmaz P, Gerken J, Schweer T, Yarza P, Peplies J, Glockner F O. 2013. The SILVA ribosomal RNA gene database project: Improved data processing and web-based tools. *Nucleic Acids Research*, **41**, D590–D596.
Rees D O, Crick P J, Jenkins G J, Wang Y, Griffiths W J, Brown T H, Al-Sarireh B. 2017. Comparison of the composition of bile acids in bile of patients with adenocarcinoma of the pancreas and benign disease. *Journal of Steroid Biochemistry and Molecular Biology*, **174**, 290–295.
Salva-Pastor N T, Chávez-Tapia N C, Uribe M, Nuño-Lámbarr N. 2019. Understanding the association of polycystic ovary syndrome and nonalcoholic fatty liver disease. *The Journal of Steroid Biochemistry and Molecular Biology*, **194**, 105445.
Segata N, Izard J, Waldron L, Gevers D, Miropolsky L, Garrett W S, Huttenhower C. 2011. Metagenomic biomarker discovery and explanation. *Genome Biology*, **12**, R60.
Sharpe L J, Brown A J. 2013. Controlling cholesterol synthesis beyond 3-hydroxy-3-methylglutaryl-CoA reductase (HMGCR). *Journal of Biological Chemistry*, **288**, 18707–18715.
Suzuki M T, Taylor L T, DeLong E F. 2000. Quantitative analysis of small-subunit rRNA genes in mixed microbial populations *via* 5'-nuclease assays. *Applied and Environmental Microbiology*, **66**, 4605–4614.
Tang B, Tang L, Li S, Liu S, He J, Li P, Wang S, Yang M, Zhang L, Lei Y, Tu D, Tang X, Hu H, Ouyang Q, Chen X, Yang S. 2023. Gut microbiota alters host bile acid metabolism to contribute to intrahepatic cholestasis of pregnancy. *Nature Communications*, **14**, 1305.
Tania M, Khan M A, Song Y. 2010. Association of lipid metabolism with ovarian cancer. *Current Oncology*, **17**, 6–11.
Therdtatha P, Song Y, Tanaka M, Mariyatun M, Almunifah M, Manurung N E P, Indriarsih S, Lu Y, Nagata K, Fukami K, Ikeda T, Lee Y K, Rahayu E S, Nakayama J. 2021. Gut microbiome of indonesian adults associated with obesity and type 2 diabetes: A cross-sectional study in an Asian city, Yogyakarta. *Microorganisms*, **9**, 897.
Tsafriri A, Chun S Y, Zhang R, Hsueh A J W, Conti M. 1996. Oocyte maturation involves compartmentalization and opposing changes of cAMP levels in follicular somatic and germ cells: Studies using selective phosphodiesterase inhibitors. *Developmental Biology*, **178**, 393–402.
Tu H, Okamoto A Y, Shan B. 2000. FXR, a bile acid receptor and biological sensor. *Trends in Cardiovascular Medicine*, **10**, 30–35.
Vazquez-Moreno M, Perez-Herrera A, Locia-Morales D, Dizzel S, Meyre D, Stearns J C, Cruz M. 2021. Association of gut microbiome with fasting triglycerides, fasting insulin and obesity status in Mexican children. *Pediatric Obesity*, **16**, e12748.
Vicente J S, Marco-Jimenez F, Perez-Garcia M, Naturil-Alfonso C, Penaranda D S, Viudes-de-Castro M P. 2022. Oocyte quality and *in vivo* embryo survival after ovarian stimulation in nulliparous and multiparous rabbit does. *Theriogenology*, **189**, 53–58.
Wahlstrom A, Sayin S I, Marschall H U, Backhed F. 2016. Intestinal crosstalk between bile acids and microbiota and its impact on host metabolism. *Cell Metabolism*, **24**, 41–50.
Wang L Y, Wang N, Le F, Li L, Lou H Y, Liu X Z, Zheng Y M, Qian Y Q, Chen Y L, Jiang X H, Huang H F, Jin F. 2015. Superovulation induced changes of lipid metabolism in ovaries and embryos and its probable mechanism. *PLoS ONE*, **10**, e0132638.
Wang Y, Xu L, Sun X, Wan X, Sun G, Jiang R, Li W, Tian Y, Liu X, Kang X. 2020. Characteristics of the fecal microbiota of high- and low-yield hens and effects of fecal microbiota transplantation on egg production performance. *Research in Veterinary Science*, **129**, 164–173.

Wei R, Han C, Deng D, Ye F, Gan X, Liu H, Li L, Xu H, Wei S. 2021. Research progress into the physiological changes in metabolic pathways in waterfowl with hepatic steatosis. *British Poultry Science*, **62**, 118–124.

Wei Z H, Li P C, Huang S J, Lkhagvagarav P, Zhu M Q, Liang C Y, Jia C L. 2019. Identification of key genes and molecular mechanisms associated with low egg production of broiler breeder hens in ad libitum. *BMC Genomics*, **20**, 408.

Welch C L, Bretschger S, Wen P Z, Mehrabian M, Latib N, Fruchart-Najib J, Fruchart J C, Myrick C, Lusis A J. 2004. Novel QTLs for HDL levels identified in mice by controlling for *Apoa2* allelic effects: Confirmation of a chromosome 6 locus in a congenic strain. *Physiological Genomics*, **17**, 48–59.

Wen C, Li Q, Lan F, Li X, Li G, Yan Y, Wu G, Yang N, Sun C. 2021. Microbiota continuum along the chicken oviduct and its association with host genetics and egg formation. *Poultry Science*, **100**, 101104.

Wild R A, Rizzo M, Clifton S, Carmina E. 2011. Lipid levels in polycystic ovary syndrome: Systematic review and meta-analysis. *Fertility and Sterility*, **95**, 1073-1079.e11.

Wu L L Y, Dunning K R, Yang X, Russell D L, Lane M, Norman R J, Robker R L. 2010. High-fat diet causes lipotoxicity responses in cumulus-oocyte complexes and decreased fertilization rates. *Endocrinology*, **151**, 5438–5445.

Xiao L, Pan G. 2017. An important intestinal transporter that regulates the enterohepatic circulation of bile acids and cholesterol homeostasis: The apical sodium-dependent bile acid transporter (SLC10A2/ASBT). *Clinics and Research in Hepatology and Gastroenterology*, **41**, 509–515.

Yang X, Wu R, Qi D, Fu L, Song T, Wang Y, Bian Y, Shi Y. 2021. Profile of bile acid metabolomics in the follicular fluid of PCOS patients. *Metabolites*, **11**, 845.

Yang Z Q, Zhang C H, Wang J P, Celi P, Ding X M, Bai S P, Zeng Q F, Mao X B, Zhuo Y, Xu S Y, Yan H, Zhang K Y, Shan Z G. 2020. Characterization of the intestinal microbiota of broiler breeders with different egg laying rate. *Frontiers in Veterinary Science*, **7**, 599337.

Yin H, Huang J, Hu M. 2022. Moderate-intensity exercise improves endothelial function by altering gut microbiome composition in rats fed a high-fat diet. *Journal of Nippon Medical School*, **89**, 316–327.

Yu J, Zhang Y, Zhu Y, Li Y, Lin S, Liu W, Tao T. 2023. Circulating bile acid profile characteristics in PCOS patients and the role of bile acids in predicting the pathogenesis of PCOS. *Frontiers in Endocrinology*, **14**, 1239276.

Yu X H, Qian K, Jiang N, Zheng X L, Cayabyab F S, Tang C K. 2014. ABCG5/ABCG8 in cholesterol excretion and atherosclerosis. *Clinica Chimica Acta*, **428**, 82–88.

Yuan T, Li J, Wang Y, Li M, Yang A, Ren C, Qi D, Zhang N. 2022. Effects of zearalenone on production performance, egg quality, ovarian function and gut microbiota of laying hens. *Toxins*, **14**, 653.

Zaefarian F, Abdollahi M R, Cowieson A, Ravindran V. 2019. Avian liver: The forgotten organ. *Animals*, **9**, 63.

Zeng Q, Li D, He Y, Li Y, Yang Z, Zhao X, Liu Y, Wang Y, Sun J, Feng X, Wang F, Chen J, Zheng Y, Yang Y, Sun X, Xu X, Wang D, Kenney T, Jiang Y, Gu H, *et al.* 2019. Discrepant gut microbiota markers for the classification of obesity-related metabolic abnormalities. *Science Reports*, **9**, 13424.

Zhang Z, Liu H, Yu B, Tao H, Li J, Wu Z, Liu G, Yuan C, Guo L, Cui B. 2020. Lycium barbarum polysaccharide attenuates myocardial injury in high-fat diet-fed mice through manipulating the gut microbiome and fecal metabolome. *Food Research International*, **138**, 109778.

Zheng X, Chen T, Jiang R, Zhao A, Wu Q, Kuang J, Sun D, Ren Z, Li M, Zhao M, Wang S, Bao Y, Li H, Hu C, Dong B, Li D, Wu J, Xia J, Wang X, Lan K, *et al.* 2021. Hyocholic acid species improve glucose homeostasis through a distinct TGR5 and FXR signaling mechanism. *Cell Metabolism*, **33**, 791-803.e797.

Zhou X, Stephens M. 2012. Genome-wide efficient mixed-model analysis for association studies. *Nature Genetics*, **44**, 821–824.

Zhou Z, Zheng Z, Xiong X, Chen X, Peng J, Yao H, Pu J, Chen Q, Zheng M. 2021. Gut microbiota composition and fecal metabolic profiling in patients with diabetic retinopathy. *Frontiers in Cell and Developmental Biology*, **9**, 732204.

Executive Editor-in-Chief Kui Li
Managing Editor Yanyan Sun